IEEE Access
Multidisciplinary | Rapid Review | Open Access Journal

Received September 25, 2019, accepted October 5, 2019, date of publication October 10, 2019, date of current version October 22, 2019.

Digital Object Identifier 10.1109/ACCESS.2019.2946258

AC Surface Flashover and Gas Generation Difference of the Cellulose Insulation Pressboard Immersed in Novel 3-Element Mixed Oil and Mineral Oil

XIN CHEN, JIAN HAO, (Member, IEEE), RUIJIN LIAO, (Member, IEEE), JIAN LI, (Member, IEEE), LIJUN YANG, (Member, IEEE), AND DAWEI FENG
State Key Laboratory of Power Transmission Equipment & System Security and New Technology, Chongqing University, Chongqing 400044, China

Corresponding author: Jian Hao (haojian2016@cqu.edu.cn)

This work was supported in part by the National Key Research and Development Program of China under Grant 2017YFB0902704, in part by the Science and Technology Project of the State Grid Corporation of China (Research on key technology for mixed insulation oil transformer), and in part by the Joint Funds of the National Natural Science Foundation of China under Grant U1866603.

ABSTRACT Surface flashover fault is one of the most challenge issues in oil-cellulose insulation pressboard system used in power transformer. In this study, a comparative study of the AC surface flashover properties of the novel 3-element mixed oil-cellulose insulation pressboard (3EMO-IP) and mineral oil-cellulose insulation pressboard (MO-IP) was performed under needle-plate and finger-finger electrode, respectively, measurement including dielectric property, surface flashover voltage, damage of cellulose pressboard surface and the gas generation behaviors after multiple surface flashover. Results show that the cellulose insulation pressboard immersed in the novel 3-element mixed insulation oil (3EMO) has higher relative permittivity and dielectric loss factor at 50 Hz, and also has slightly lower surface resistivity. The AC surface flashover voltage of the 3EMO-IP is higher than that of MO-IP under needle-plate and finger-finger electrode (electrode distance 5 mm, 10 mm, 15 mm and 20 mm). Compared to MO-IP, the lower electric field intensity at the oil-pressboard interface, as well as more difficult for surface charge accumulation of 3EMO-IP and the higher breakdown voltage of 3EMO lead to the higher AC surface flashover voltage of 3EMO-IP. Moreover, the carbonization of fibers in 3EMO-IP is slightly less. After multiple surface flashover, C_2H_2 and total hydrocarbon gases are the main differences between 3EMO-IP and MO-IP, which is more marked with the increase of flashover times. This study offers a reference for improving the surface flashover property of oil-pressboard insulation system by using 3EMO.

INDEX TERMS Surface flashover, mixed oil, cellulose insulation pressboard, dielectric property, surface damage, dissolved gas.

I. INTRODUCTION

Polymer insulation materials, such as cellulose, are widely used in high-voltage equipment as electrical insulation [1]. The cellulose products (pressboard, kraft paper, etc.) and insulating oil constitute the compound insulation systems in oil-immersed transformer and its property directly affects the safe operation of transformer [2], [3]. Insulating oil has a significant impact on the performance of oil-paper insulation system, which is regarded as the ''blood'' of transformer. Among all types of oils, mineral oil (MO) has a long history of application in transformer because of its low price and good insulation properties. However, the poor fire performance and biodegradability of mineral oil makes it inconsistent with the development of electric equipment [4], [5]. As a promising alternative for mineral oil, natural esters are not only renewable and biodegradable, but also can delay the aging of cellulose [6]–[9]. However, some defects, such as poor oxidation stability and high kinematic viscosity, are needed to be improved [10], [11].

Mixed oil developed from mineral oil and natural ester retains the good physical and electrical properties of mineral oil, and also absorbs the advantages of natural ester on fire resistance and anti-aging properties. Therefore, extensive

The associate editor coordinating the review of this manuscript and approving it for publication was Boxue Du.

researches on mixed oil has been carried out and the heat of these studies have been on rising trend in recent years [12]–[15]. In 2012 and 2015, our team proposed two types of mixed insulation oil, which mixed mineral oil and olive oil/rapeseed oil at 4:1 in volume ratio, respectively [12], [13]. Aside from the ability to delay the aging of insulation paper, their fire points and flashpoints are satisfied. In 2017, Takahashi et al. presented their results on the negative discharge response of mixed insulation oil, which was composed of 80% vegetable oil and 20% mineral oil in their work [14]. In 2018, Abderrahmane Beroual et al. proposed a mixture of 20% Jatropha methyl ester oil and 80% mineral oil [15]. Its average AC breakdown voltage and DC breakdown voltage of the mixed oil increased by 12.0% and 28.5% compared to mineral oil [15].

However, some key parameters of existed mixed insulation oils, such as kinematic viscosity and dielectric loss factor, failed to meet the mineral oil standard IEC 60296: 2012. In order to apply the mixed oil directly in the mineral oil transformer without structural changes, it is necessary to develop a novel mixed insulation oil that meets the mineral oil standard. To solve this problem, our team proposed a novel 3-element mixed insulation oil (3EMO), which is prepared by mixing mineral oil, soybean oil and palm oil in a volume ratio at 76:19:5 with compound antioxidant (0.2 wt% T511 + 0.2 wt% L06) [16]. Its parameters satisfies the requirements of IEC 60296:2012. 3EMO can be a proper alternative for MO with good physicochemical, insulation and anti-aging performance [16], [17].

The surface flashover between insulating oil and cellulose pressboard is a common fault of transformer [18]–[20]. The surface flashover at oil-pressboard interface can lead to the partial or total deterioration of insulation. At present, the researches on surface flashover characteristics are mainly aimed at mineral oil-cellulose insulation pressboard (MO-IP) and esters-cellulose insulation pressboard [18]–[23]. In order to ensure the safe operation of the traditional mineral oil transformer filled with 3EMO, it is essential to well understand the surface flashover characteristics of the novel 3-element mixed oil-cellulose insulation pressboard (3EMO-IP). In this way, 3EMO could be safely used in transformer.

In this paper, taking MO-IP as reference, the surface flashover experiment was carried out on 3EMO-IP using ''needle-plate'' and ''finger-finger'' electrode, respectively. Firstly, the surface flashover characteristics under different electrode distance was studied. Secondly, the discharge damages on the surface of cellulose pressboard was analyzed. Finally, the concentrations of the fault characteristic gases dissolved in oil after multiple surface flashover was measured.

II. EXPERIMENTS

A. MATERIALS AND SAMPLE PREPARATION

The cellulose insulation pressboard utilized in this experiment were provided by Yadongya Transformer Company Chongqing, China. Its density and thickness are 1.2 g/cm^3 and 0.45 mm, respectively. Karamay 25# naphthenic mineral oil was used in experiment as reference. 3EMO was prepared by mixing mineral oil, soybean oil and palm oil in a volume ratio at 76:19:5, and 0.4 wt% compound antioxidant (0.2 wt% T511 and 0.2 wt% L06) were also added. The main parameters of the two insulation oils are listed in TABLE 1. The cellulose pressboard was dried at 90 °C/50 Pa for 48 h, and immersed in MO and 3EMO at 60 °C/50 Pa for 24 h to complete the oil-impregnation process, respectively. The moisture contents of the oil-impregnated insulation pressboard is below 1%.

TABLE 1. Parameters of 3EMO and MO.

Parameters	3EMO	MO
Kinematic viscosity (40 °C, mm^2/s)	11.65	9.2
Moisture content (ppm)	14	11
Breakdown voltage (2.5 mm, kV)	78.6	72
Density (20 °C, kg/m^3)	886.8	890
tan δ (90 °C)	0.0047	0.001
Acid value (mg KOH/g)	0.007	0.004
Relative permittivity(90 °C)	2.32	2.12

B. DIELECTRIC PROPERTY TEST OF OIL IMPREGNATED PRESSBOARD

Novocontrol Concept 80 Broadband Dielectric Spectroscopy Equipment was used in dielectric test for oil-impregnated pressboard from $10^{-1} \sim 10^6$ Hz. The test temperature was 90 °C. In order to reflect the conductive properties of the oil-pressboard interface, surface conductivity of MO-IP and 3EMO-IP was measured by Keithley 6517B and 8009 resistivity test fixture according to IEC 60093. The DC supply voltage was set at 100 V, and the experimental temperature was 25 °C. Surface conductivity of each oil- impregnated pressboard was measured for 10 minutes and recorded every 30 s. Every sample was tested three times, and the average surface conductivity of oil-impregnated pressboard was analysed at here.

C. SURFACE FLSHOVER VOLTAGE, SURFACE DAMAGE AND DISSOLVED GAS TEST

The surface flashover experimental equipment is shown in Fig. 1. The test cell contains two electrode structures, which are the needle-plate and finger-finger electrodes made by copper. In the internal structure of the transformer, slightly un-uniform electric field exist between adjacent windings, the low-voltage winding and the core shield, while the extremely un-uniform electric field is the most common electric field in transformer. Therefore, needle-plate electrode and finger-finger electrode are used in this experiment to simulate extremely un-uniform electric field and slightly un-uniform electric field, respectively, in order to study the

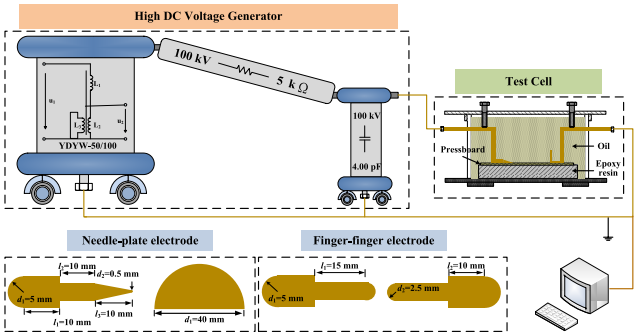

FIGURE 1. The surface flashover test for oil-pressboard system.

surface flashover characteristics of 3EMO-IP and MO-IP. The detailed dimension of the electrodes is shown in Fig. 1. The experimental temperature was 25 °C, and the internal fluid volume of test cell controlled at 1.5 L to completely impregnate the electrode. Each kind of electrode has been processed before experiment according to the same specifications. After every 20 times of flashover, new electrodes will be used to reduce the influence of shape changes on the experiment.

The oil-impregnated pressboard was removed from oil and placed on the epoxy block. The electrodes were placed with axis coincidence, and the distance between the electrodes was set at planned value. After the dried insulating oil was filled into the plexiglass test cell, the bolts above the electrode were adjusted to closely fit the electrode and pressboard. Firstly, surface flashover voltage of MO-IP and 3EMO-IP were obtained under needle-plate and finger-finger electrode, respectively. The distances of oil gap between positive and negative electrode varied from 5 mm up to 20 mm with 5 mm increment. The rise rate of AC voltage was controlled at 3 kV/s, and each sample was tested 15-18 times. Secondly, after 30 times flashover at 10 mm oil gap under needle-plate and finger-finger electrode, the surface damage of cellulose insulation pressboard was studied by microscope. The observation position focused on the pressboard surface at the tip of needle and finger electrode, and the microscope was OLYMPUS-BX53 at the magnification of 10×. Thirdly, after 3, 5, 10, 15 and 20 times flashover, the concentrations of characteristic gases dissolved in oils were detected by gas chromatography to analyse the difference on gas production characteristics between 3EMO-IP and MO-IP.

III. RESULTS AND DISCUSSIONS

A. DIELECTRIC PROPERTY OF OIL IMPREGNATED PRESSBOARD

The relative permittivity of oil-impregnated pressboard decrease with frequency gradually, and 3EMO-IP has higher relative permittivity than MO-IP, especially when the frequency is less than 20 Hz. as Fig. 2(a) shows. This difference mainly due to the polarity property of two oil molecules, as shown in Fig. 3. Because the main component of vegetable oil is triglyceride, its polarization type is mainly turning-direction polarization of dipole under electric field, while

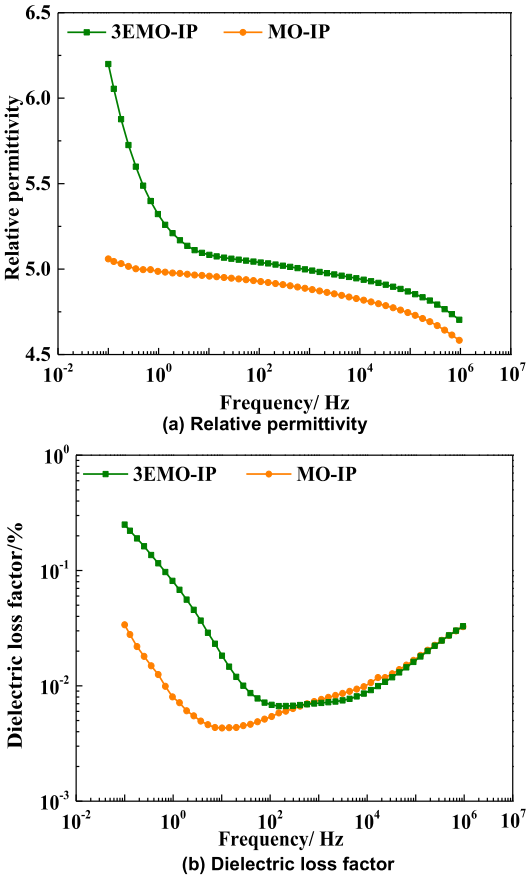

FIGURE 2. The dielectric properties of mixed oil impregnated pressboard and mineral oil impregnated pressboard.

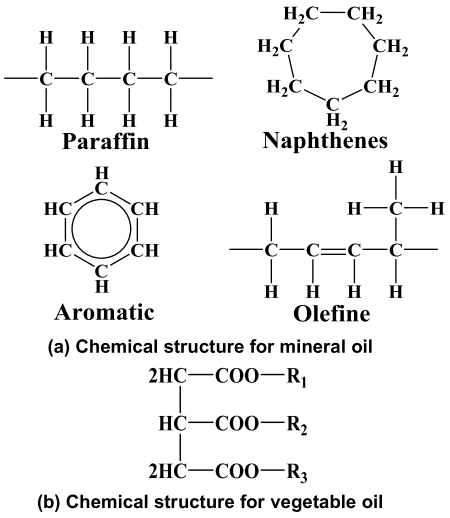

FIGURE 3. Chemical structure for mineral oil molecule and vegetable oil molecule.

the displacement polarization of electron is dominant for mineral oil molecule under the electric field because of its small dipole moment. The turning-direction polarization of dipole is much greater than the displacement polarizability of electron. So 3EMO has higher relative permittivity than MO, which results in the higher relative permittivity of 3EMO-IP.

With the increase of frequency, the dielectric loss factors of two oil-impregnated insulation pressboards is down first and up later gradually, as shown in Fig.2(b). The dielectric loss factor of 3EMO-IP reach 0.019% at power frequency, which is 2.38 times higher than MO-IP. The dielectric loss factor of 3EMO-IP is higher than that of MO-IP in most frequency ranges, and the dielectric loss factor can be obtained by Equation (1) [24].

$$\tan\delta = [\frac{r}{\omega\varepsilon_0} + (\varepsilon_s - \varepsilon_\infty)\frac{\omega\tau}{1+\omega^2\tau^2}]/(\varepsilon_\infty + \frac{\varepsilon_s - \varepsilon_\infty}{1+\omega^2\tau^2}) \tag{1}$$

where r is the conductivity of oil-impregnated insulation pressboard; τ is the time constant of relaxation polarization; ε_s and ε_∞ are the static permittivity and optical permittivity of oil-impregnated insulation pressboard, respectively. When $\omega\tau << 1$, the dielectric loss factor can be as equation (2). The dielectric loss in the low-frequency range is mainly caused by conductivity loss, which shows downtrend with the increase of frequency. As the frequency continues to rise, the period of the alternating electric field is gradually close to the relaxation polarization time when $\omega\tau$ is close to 1. With the increase of the polarization loss, the growth rate of the active current of the oil-impregnated insulation pressboard exceed that of the reactive current, which result in the increase of the dielectric loss factor with frequency.

$$\tan\delta = \frac{r}{\omega\varepsilon_0\varepsilon_s} \tag{2}$$

According to the description of the relationship between dielectric loss and frequency, there is a minimum of the dielectric loss factor during the increase of frequency. Due to the higher conductivity of 3EMO, 3EMO-IP has higher dielectric loss factor than MO-IP, as shown in low-frequency range of Fig.2. The strong polarity of the mixed oil molecules result in its smaller time constant of relaxation polarization, compared with mineral oil molecules. Therefore, the frequency corresponding to the minimum of dielectric loss factor is higher for 3EMO-IP. During the 10 Hz to 10^2 Hz, the dielectric loss factor of MO-IP is in an upswing, while the dielectric loss factor of 3EMO-IP is still decline with increase of frequency at this range. So the difference between the two samples gradually narrow, and even the dielectric loss factor of MO-IP reverse during 10^3 Hz to 10^5 Hz. As the frequency continues to rise up to 10^5 Hz, the dielectric loss of both samples reaches a very high level, and the difference in polarization loss caused by molecular polarity disappears.

Fig. 4 is the surface resistivity of 3EMO-IP and MO-IP. It shows that the surface resistivity of 3EMO-IP is lower than that of MO-IP, and reaches $5.25\times10^{14}\Omega$ and $5.98\times10^{14}\Omega$ after 1 min of voltage application. The difference in surface resistivity between 3EMO-IP and MO-IP can be explained by volume resistivity of oils. Due to the higher volume resistivity of MO, the surface resistivity of 3EMO-IP is lower than that of MO-IP. With the increase of test time, the difference on surface resistivity between two kinds of oil impregnated pressboards decreases continuously. After 7 min they are nearly the same.

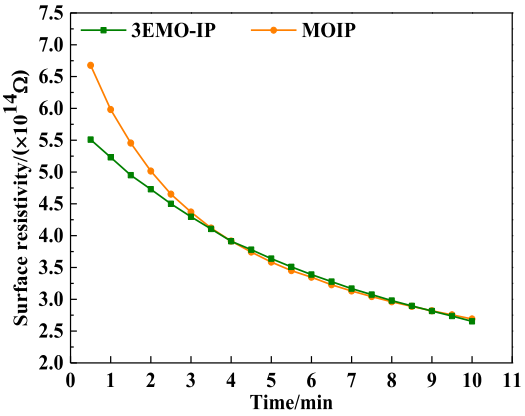

FIGURE 4. The surface resistivity of mixed oil impregnated pressboard and mineral oil impregnated pressboard.

B. SURFACE FLSHOVER VOLTAGE OF OIL-CELLULOSE INSUALTION PRESSBOARD UNDER NEEDLE-PLATE AND FINGER-FINGER ELECTRODE

1) SURFACE FLASHOVER VOLTAGE

The surface flashover voltage under needle-plate electrode and finger-finger electrode at different electrode distance were fitted with the two-parameter Weibull distribution function, whose probability density function and failure probability are shown in Equation (3), where λ is the scale parameter, and k is the shape parameter; P_F is the probability of failure, i is the rank of a sample, and n is the number of samples.

$$f(x;\lambda,k) = \begin{cases} \frac{k}{\lambda}\left(\frac{x}{\lambda}\right)^{k-1} e^{-(x/\lambda)^k} & x \geq 0 \\ 0 & x < 0 \end{cases} \tag{3}$$

$$P_F = \frac{i-0.3}{n+0.4} \times 100\% \tag{4}$$

The Weibull distribution of surface flashover voltage for the 3EMO-IP and MO-IP under needle-plate electrode at different oil gap distance is presented in Fig. 5. The R-Square(R^2) of each Weibull distribution obtained by linear fitting is also shown in TABLE 2. As the oil gap between needle electrode and plate electrode increases, the Weibull distribution line moves from left to right direction. This means that the surface flashover voltages of the two kinds of oil-cellulose insulation pressboard show upward trend. The values of R^2 were basically above 0.85, which demonstrate the surface flashover voltage was fitted with the two-parameter Weibull distribution, and the equivalent surface flashover voltage values can be obtained at any certain failure probability.

In order to compare the surface flashover voltage of pressboard immersed in 3EMO and MO clearly, the equivalent surface flashover voltages at 5% probability in the Weibull distribution and the average values are shown in TABLE 2 and Fig. 6. Compared with MO-IP, the surface flashover

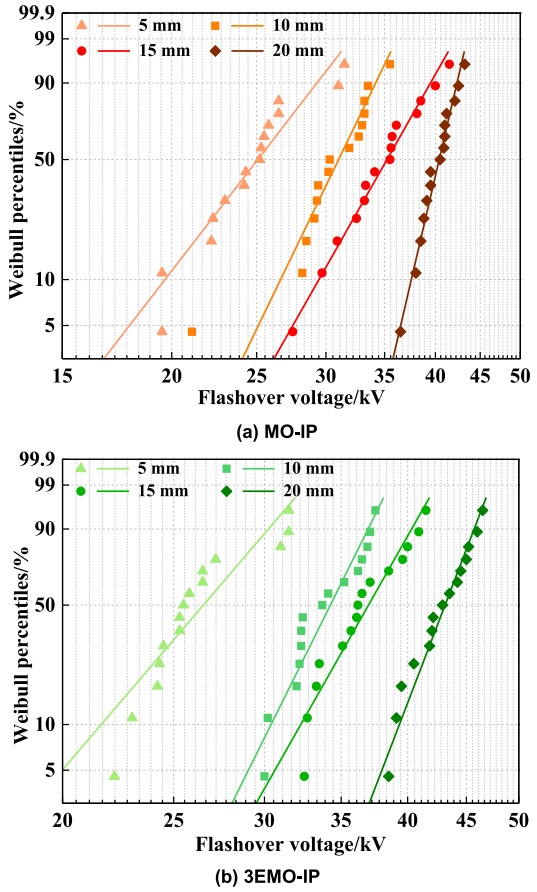

FIGURE 5. Weibull distributions of surface flashover voltages under needle-plate electrode.

TABLE 2. The equivalent flashover voltages at 5% probability and average values of 3EMO-IP and MO-IP under needle-plate electrode.

Gap/mm	3EMO-IP			MO-IP		
	U_{AVG}/kV	$U_{5\%}$/kV	R^2	U_{AVG}/kV	$U_{5\%}$/kV	R^2
5	26.29	20.05	0.86	24.82	17.88	0.89
10	33.17	29.08	0.96	30.61	25.09	0.79
15	36.81	31.68	0.97	34.81	27.44	0.96
20	42.22	38.08	0.98	40.15	36.41	0.96

of 3EMO-IP occurs at higher voltage. Take the result at oil gap 10 mm as an example, the flashover voltage at 5% probability and average values of 3EMO-IP is 15.90% and 8.36% higher than those of MO-IP, respectively.

The Weibull distribution of surface flashover voltage of 3EMO-IP and MO-IP under finger-finger electrode are presented in Fig. 7. Similar to the needle-plate electrode, the surface flashover voltage of oil-cellulose insulation pressboard has a significant increase with the distance of oil gap. Fig. 8 and TABLE 3 show the equivalent surface flashover voltages at 5% probability and the average values. Compared with MO-IP, 3EMO-IP has higher flashover voltage at the same oil gap. For instance, for 3EMO-IP, its equivalent flashover voltages at 5% probability are 1.05 and 1.07 times higher than those of MO-IP at 10 mm and

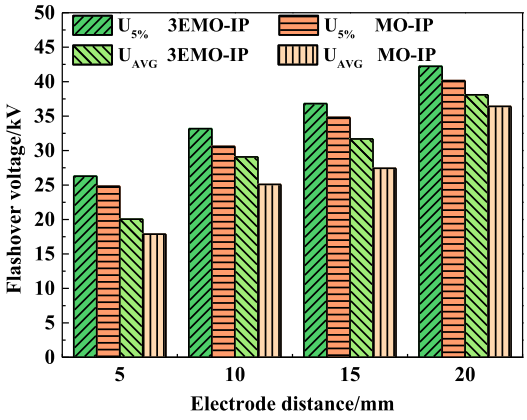

FIGURE 6. Comparison of surface flashover voltages under needle-plate electrode between 3EMO-IP and MO-IP.

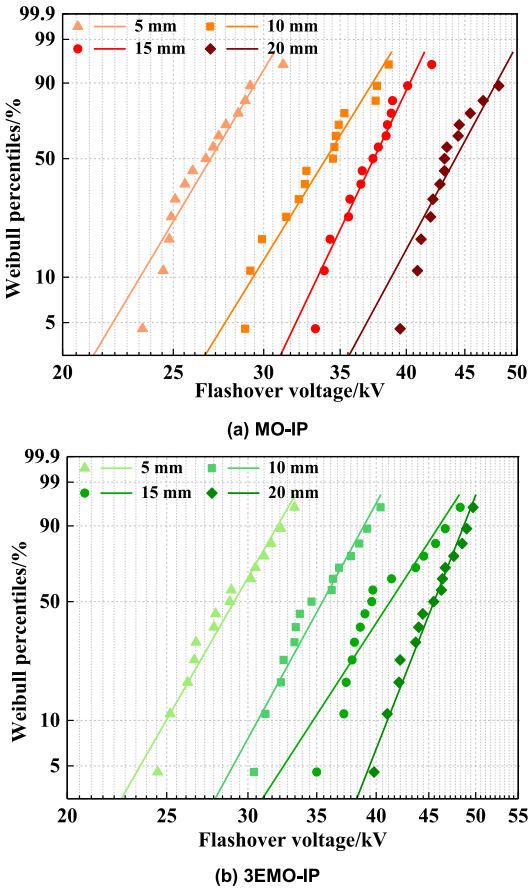

FIGURE 7. Weibull distributions of surface flashover voltages under finger-finger electrode.

20 mm, as shown in Fig. 8. Besides, the difference in surface flashover voltage between MO-IP and 3EMO-IP is more significant under needle-plate electrode. According to the average of the differences between MO-IP and 3EMO-IP at the four gap distances, the equivalent flashover voltage of 3EMO-IP is 12.02% higher than that of MO-IP under needle-plate electrode, while this number decrease to 4.91% under finger-finger electrode.

TABLE 3. The equivalent flashover voltages at 5% probability and average values of 3EMO-IP and MO-IP under finger-finger electrode.

Gap/mm	3EMO-IP			MO-IP		
	U_{AVG}/kV	$U_{5\%}$/kV	R^2	U_{AVG}/kV	$U_{5\%}$/kV	R^2
5	28.77	23.57	0.99	26.75	22.14	0.96
10	35.11	29.05	0.98	33.65	27.75	0.97
15	40.85	32.52	0.84	37.19	31.96	0.96
20	45.13	39.39	0.98	43.89	36.90	0.88

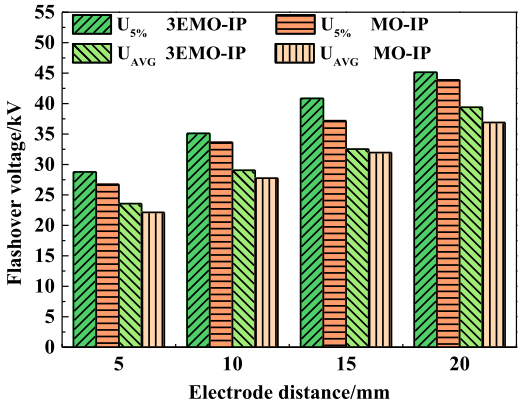

FIGURE 8. Comparison of surface flashover voltages under finger-finger electrode between 3EMO-IP and MO-IP.

2) BREAKDOWN VOLTAGE OF OIL GAP

The streamer develops in insulating oil, along the oil-pressboard interface. So the breakdown property of insulating oil is also an essential factor for surface flashover process. The Weibull distribution of breakdown voltage for 3EMO and MO under needle-plate electrode and finger-finger electrode are presented in Fig. 9, and the oil gap between positive and negative electrode was set at 10 mm and 20 mm, respectively. The equivalent surface flashover voltages at 5% probability and the average values are shown in TABLE 4. Due to the greater distortion of the electric field, 3EMO and MO have lower breakdown voltages under needle-plate electrode than those under finger-finger electrode. Compared with MO, the breakdown voltage of 3EMO is higher, which is an important reason for higher surface flashover voltage of 3EMO-IP.

TABLE 4. The equivalent breakdown voltages at 5% probability and average values of 3EMO and MO.

Electrode	Gap /mm	3EMO			MO		
		U_{AVG}/kV	$U_{5\%}$/kV	R^2	U_{AVG}/kV	$U_{5\%}$/kV	R^2
Needle-plate	10	36.39	30.45	0.96	33.91	28.50	0.79
electrode	20	45.97	38.75	0.98	43.34	35.93	0.96
Finger-finger	10	39.43	34.77	0.98	38.09	32.36	0.97
electrode	20	49.89	43.42	0.98	47.63	40.90	0.88

3) SURFACE FLASHOVER DIFFERENCE ANALYSIS

The distribution of electric field strength between insulating oil and insulating paperboard can be calculated in

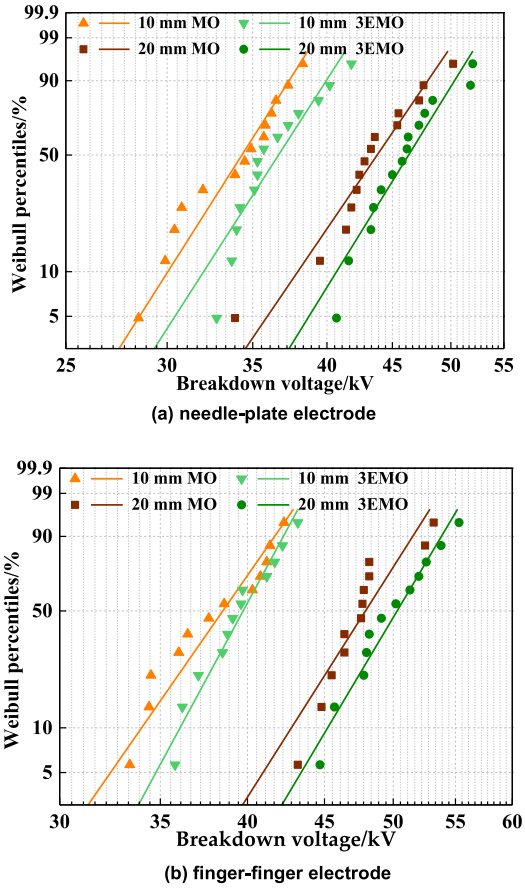

FIGURE 9. Weibull distributions of breakdown voltages under needle-plate and finger-finger electrode.

equation (5) [25].

$$E_{Oil}/E_p = \varepsilon_{rp}/\varepsilon_{roil} \tag{5}$$

where ε_{roil} and ε_{rp} are the relative permittivities of insulating oil and oil-impregnated pressboard. E_{oil} and E_p are the electric field intensities of oil and insulating pressboard. Because the ratio of oil to pressboard in relative permittivity is smaller, the distortion at oil-pressboard interface in 3EMO-IP is less than that in MO-IP.

A COMSOL electric field simulation of the two kind of test electrodes for the two kinds of oil-cellulose insulation pressboard system were studied by using Electrostatic Module, and the simulation results at 0.005 s of 3EMO-IP is shown in Fig. 9. The parameters of the insulating oil and oil impregnated pressboard used in the simulation can be found in TABLE 1 and Fig. 2. The applied voltages were the AC voltages, and the amplitudes were 40 kV under needle-plate electrode and 45 kV under finger-finger electrode respectively, according to the experiment result. The two electrodes were set to AC voltage and zero potential respectively. Under needle-plate electrode, the needle electrode was connected to the high voltage, and the plate electrode was grounded. The gap of positive and negative electrode was set at 20 mm. In the three-dimensional simulation structure, the x direction and

the y direction are respectively parallel and perpendicular to the axis of the electrodes, and the z direction is perpendicular to the surface of the pressboard.

The result shows that the electric field intensity at the tip of needle electrode is significantly higher than that of finger-finger electrode, as Fig. 10 shows. The magnitude of electric field intensity (E_m), the components of electric field intensity on X-axis (E_x) and Z-axis (E_z) at the tip of needle/ finger electrode for 3EMO-IP and MO-IP were presented in TABLE 5. Whether at the tip of the needle electrode or the finger electrode, it can be concluded that E_m, E_x and E_z in 3EMO-IP are slightly lower than those in MO-IP. The lower component of electric field intensity on X-axis (E_x) means that the electric stress provided by the external electric field is relatively small during the process of streamer development, and the lower Z-axis component (E_z) also reduces the damage to the cellulose surface by weakening the interaction between the streamer and oil-impregnated pressboard.

Fig 11 shows the variation of electric field intensities along the axis of the two electrodes for 3EMO-IP and MO-IP. The distortion of the electric field are majorly at the tip of electrode, and the magnitude of electric field of MO-IP is slightly higher than that of 3EMO-IP, as shown in Fig. 11. In order to further compare the difference in electric field

TABLE 5. Magnitude of electric field intensity (E_m), the components on X-axis (Ex) and Z-axis (E_z) along oil-impregnated pressboard.

Electrode	3EMO-IP ($\times 10^7$V/m)			MO-IP($\times 10^7$V/m)		
	E_X	E_Z	E_m	E_X	E_Z	E_m
Needle-plate electrode	3.8300	1.2367	4.0247	3.9126	1.3915	4.1527
Finger-finger electrode	2.2158	0.6539	2.3128	2.2583	0.6548	2.3531

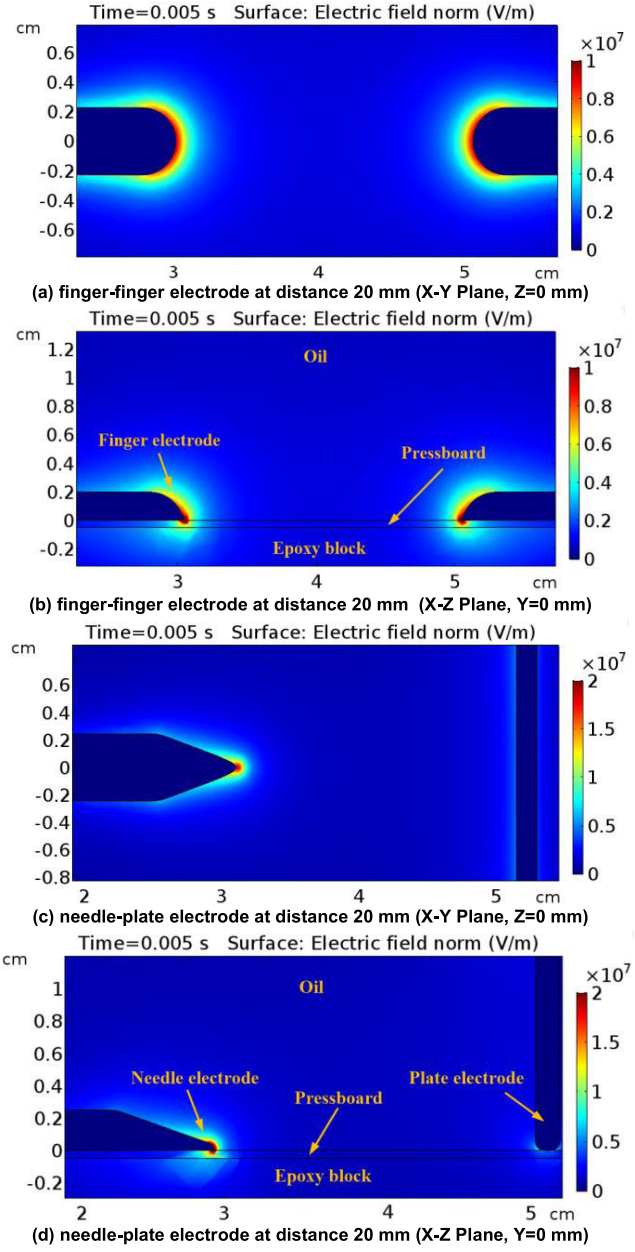

(a) finger-finger electrode at distance 20 mm (X-Y Plane, Z=0 mm)

(b) finger-finger electrode at distance 20 mm (X-Z Plane, Y=0 mm)

(c) needle-plate electrode at distance 20 mm (X-Y Plane, Z=0 mm)

(d) needle-plate electrode at distance 20 mm (X-Z Plane, Y=0 mm)

FIGURE 10. Electric field distribution simulation result of the 3EMO-IP under needle-plate electrode and finger-finger electrode.

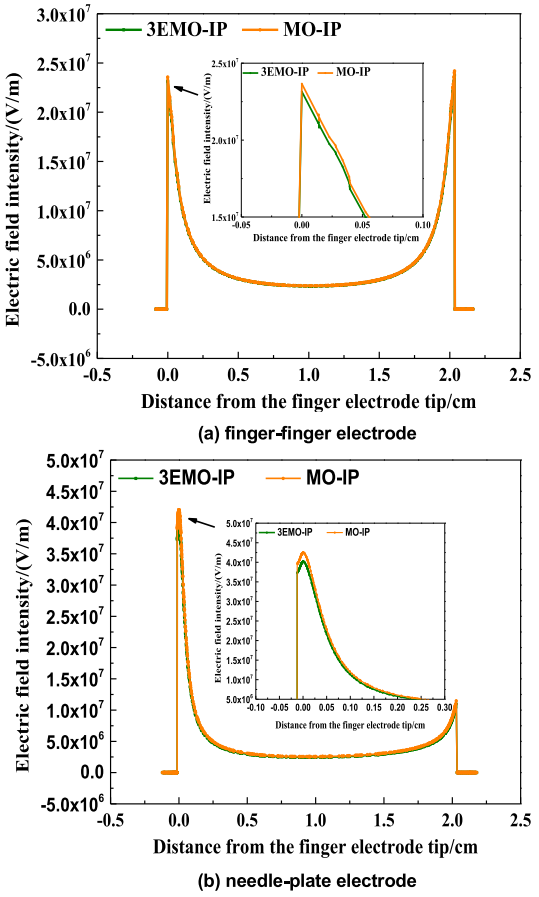

(a) finger-finger electrode

(b) needle-plate electrode

FIGURE 11. Electric field intensity along the axis of the two electrodes for 3EMO-IP and MO-IP under finger-finger electrode and needle-plate electrode.

intensity between 3EMO-IP and MO-IP, the magnitudes of electric field intensity were obtained at two points in oil and pressboard respectively, apart 0.1 mm to the oil-pressboard interface, as shown in TABLE 6. Because of lower relative permittivity for insulating oil, the electric field intensity in oil (E_o) is higher than that in pressboard (E_p). Compared with MO-IP, 3EMO-IP not only has lower electric field intensities in oil and pressboard, but also has the lower difference between E_o and E_p, which reflect the relatively uniform distribution of electric field in 3EMO-IP.

TABLE 6. Magnitudes of electric field intensity in oil and pressboard, 0.1 mm away from the oil-pressboard interface.

Electrode	3EMO/(x 10^7 V/m)			MO/(x 10^7 V/m)		
	E_o	E_p	ΔE	E_o	E_p	ΔE
Needle electrode	3.1264	2.4497	0.6767	3.2369	2.1581	1.0788
Finger electrode	1.3827	1.2910	0.0917	1.4023	1.2059	0.1964

The difference of flashover voltages between 3EMO-IP and MO-IP can also be analyzed from the interface charge. The interface charges are divided into free surface charge from the space charge, and bound surface charge from the polarization charge, as shown in Fig. 12. J.-H. Choi et al [26] studied the distribution of the charge at interface oil-pressboard. They proposed that the dominant space charge density is due to the positive ions in the streamer head, while the negative bound surface charge is dominant around the streamer head region, and the positive free surface charge remains around the back of the streamer head, as Fig. 13 shows. Because of the attraction force between space charge and bound surface charge around the streamer head, the creeping discharge developed continuously. The repulsion force around the back of the streamer head, which results in the force pushing forward.

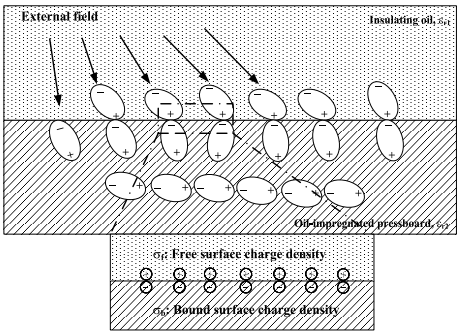

FIGURE 12. Distribution of surface charges at the interface of oil-cellulose insulation pressboard when an external field was applied [26].

Owing to these forces, faster surface discharge will be achieved with the higher electric field intensity, as shown in Fig. 13. Compared with the 3EMO-IP, there is more permittivity difference between MO and its impregnated pressboard,

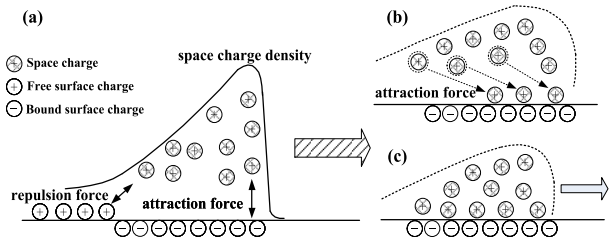

FIGURE 13. Process of creepage discharge at the oil-cellulose pressboard interface [26].

which means larger electric field concentrated at the interface of oil-pressboard. Therefore, more space charges were generated by ionization by the greater the field concentration at the interface, while the negative surface charge density at the oil-pressboard interface and the attractive force between the space charge and the surface charge increase.

Besides, the higher AC breakdown voltage of 3EMO under needle-plate electrode and finger-finger electrode is also a reason for advantage of 3EMO-IP in flashover voltage. According to the Fig. 4, 3EMO-IP also has smaller surface resistivity, which is not conducive to accumulation of surface charge during the flashover process.

C. SURFACE DAMAGE OF PRESSBOARD

During the surface flashover, the development of streamer is accompanied by the thermal process which damages the cellulose of oil-impregnated pressboard. After 30 times of surface flashover, the carbonization marks on the pressboard surface of 3EMO-IP and MO-IP are shown in Fig. 14 and Fig. 15. It is clearly that the fibers on the pressboard surface was carbonized by the discharge streamer, and surface damage under needle-plate electrode is more serious than that under finger-finger electrode. The pressboard surface damage of 3EMO-IP is slightly less than that of MO-IP after 30 times flashover.

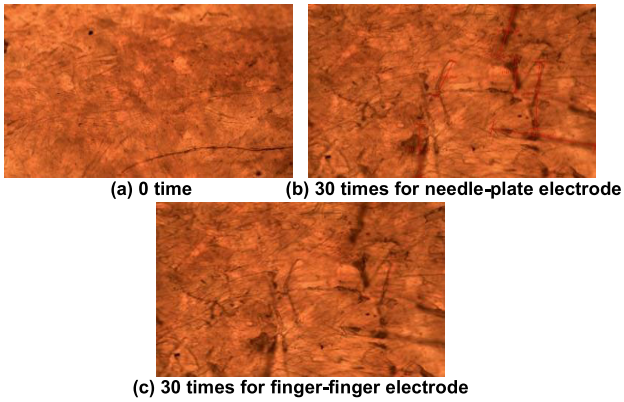

FIGURE 14. Cellulose damage of 3EMO-IP after 30 times surface flashover.

The fiber structure of the pressboard surface is surrounded by insulating oil. Better thermal stability of insulating oil

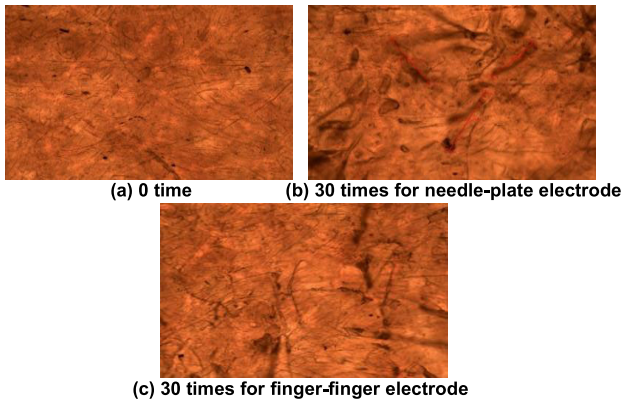

FIGURE 15. Cellulose damage of MO-IP after 30 times surface flashover.

can protect the cellulose of pressboard surface to reduce the damage during flashover process. In order to explore the thermal decomposition of 3EMO and MO, thermogravimetric test was conducted using TG Q50 produced by American TA company. The heating rate was set at 10 °C/min, and nitrogen was used to eliminate the influence of oxygen on thermal decomposition of insulating oil.

The thermogravimetric curves of 3EMO and MO are shown in Fig. 16. The decomposition rate of MO reached the maximum 1.71 %/°C at 214.19 °C. The initial decomposition temperature was 168.27 °C, and MO was completely decomposed before the temperature reached 250 °C. Compared with mineral oil, 3EMO had two peaks of decomposition rate, 1.185 %/°C at 219.29 °C and 0.305 %/°C at 387.90 °C respectively. Because of low decomposition rate and two stages of thermal decomposition, it was not until 450 °C that 3EMO was fully thermally decomposed. It can be concluded that 3EMO is more stable than MO at high temperature, thus has better protective effect on cellulose on pressboard surface during the streamer development.

D. GAS GNERATION BEHAVIORS UNDER FLASHOVER OF OIL-PRESSBOARD

Fig. 17 shows the variation of the dissolved gas contents in 3EMO and MO caused by multiple times of surface flashover in 3EMO-IP and MO-IP under needle-plate electrode. The contents of H_2 and hydrocarbon gases dissolved in oils increased significantly with flashover times, especially for H_2 and C_2H_2. Compared with three times of surface flashover, the ratios of dissolved H_2 and C_2H_2 contents to total dissolved gas content increased from 9.06% and 22.46% to 14.00% and 43.38% after twenty times flashover. Besides, after 20 times flashover, the content of total hydrocarbon accounted for 51.88% of the total dissolved gases in 3EMO

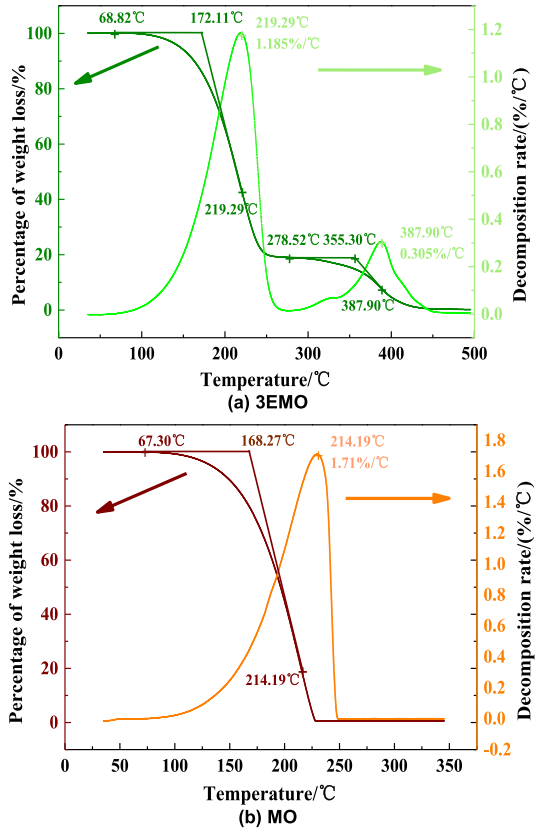

FIGURE 16. Thermogravimetric curve analysis of the 3-element mixed insulation oil and mineral oil.

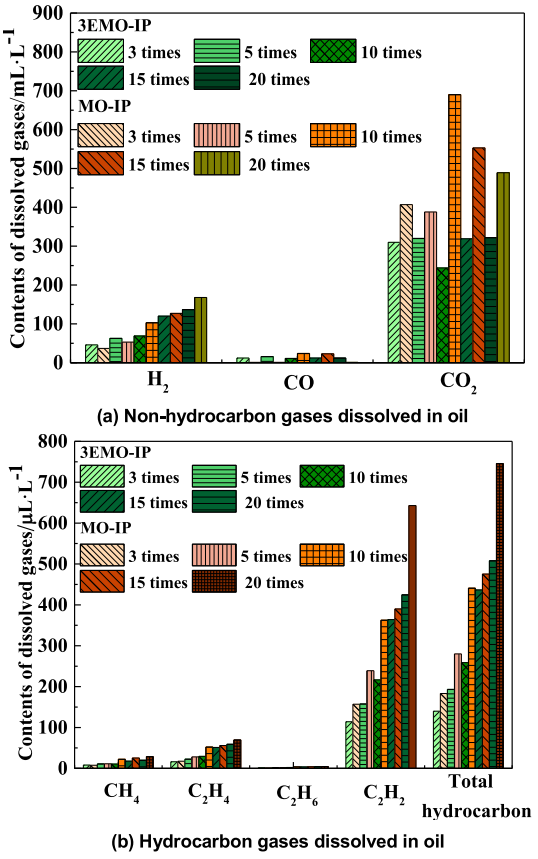

FIGURE 17. The contents of dissolved gases in oil after multiply surface flashover under needle-plate electrode.

under needle-plate electrode, while this number slightly rise to 53.12% in MO.

Fig. 18 shows the variation of the dissolved gas contents in 3EMO and MO caused by multiple times of surface flashover under finger-finger electrode. According to the dissolved gases values in Fig. 17 and Fig.18, it can be concluded the contents of characteristic gases under finger-finger electrode is higher than that under needle-plate electrode after the same times of flashover in oil-insulation cellulose pressboard system. Taking the C_2H_2 dissolved in 3EMO as an example, the content of the C_2H_2 after 20 times flashover under finger-finger electrode is 18.32% higher than that under needle-plate electrode. Compared with MO-IP, the contents of C_2H_2 and total hydrocarbon gases in 3EMO are significantly smaller, and these difference is more significant with the increase of flashover times. For instance, the contents of C_2H_2 in mineral oil is 37.54% higher than that in 3EMO after 3 times flashover, while this number rise to 51.39% higher after 20 times flashover. Moreover, the difference between the H_2 contents in 3EMO and MO is not obvious, so do CH_4 and C_2H_6.

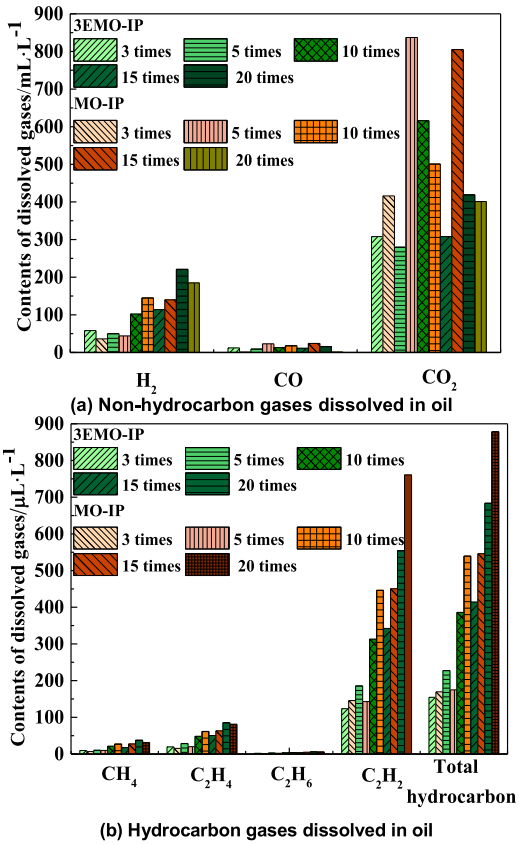

FIGURE 18. The contents of dissolved gases in oil after multiply surface flashover under finger-finger electrode.

According to IEC 60599:2015, the ratios of C_2H_2/C_2H_4, CH_4/H_2 and C_2H_4/C_2H_6 are useful method in diagnosis of transformer failures, as shown in TABLE 7 [27]. Based on the experimental data, the ratios of C_2H_2/C_2H4, CH_4/H_2 and C_2H_4/C_2H_6 for 3EMO-IP and MO-IP after multiple flashover were both satisfied with the discharge fault of low energy. The diagnosis method of surface flashover fault for mineral oil transformer is also suitable for the 3-elemnt mixed oil-insulation cellulose pressboard system.

TABLE 7. The diagnosis method of transformer failures based on dissolved gas analysis (DGA) [27].

Case	Characteristic fault	C_2H_2/C_2H_4	CH_4/H_2	C_2H_4/C_2H_6
PD	Partial discharge	NS*	<0.1	<0.2
D1	Discharges of low energy	>1	0.1-0.5	>1
D2	Discharges of high energy	0.6-2.5	0.1-1	>2
T1	Thermal fault T<300 ℃	NS*	>1 but NS*	<1
T2	Thermal fault 300 ℃<T<700 ℃	<0.1	>1	1-4
T3	Thermal fault T>700 ℃	<0.2	>1	>4

* NS=Non-significant whatever the value

IV. CONCLUSION

This paper mainly focuses on the comparative study of the AC surface flashover properties of 3EMO-IP and MO-IP, including surface flashover voltage, the damage of cellulose pressboard surface and the gas generation behaviors after surface flashover. The main conclusions are listed as follows:

(1) 3EMO-IP has slightly higher relative permittivity and dielectric loss factor than those of MO-IP at 50 Hz due to the difference in oil molecular polarity. With the increase of test time, the difference on surface resistivity between two kinds of oil impregnated pressboards decreases continuously until they are nearly the same.

(2) The surface flashover voltage increases with the oil gap distance for both 3EMO-IP and MO-IP under needle-plate and finger-finger electrode, respectively. The surface flashover voltage of 3EMO-IP is higher than that of MO-IP. Higher breakdown voltage of 3EMO is a reason for this advantage. Lower electric field intensities in 3EMO-IP and more uniform distribution of electric field between oil and pressboard also result in the higher flashover voltage of 3EMO-IP. Besides, the lower surface resistivity of 3EMO-IP is not conducive to the accumulation of interface charge to improve flashover voltage.

(3) After 30 times flashover at the interface of oil-cellulose pressboard, the carbonization of surface fibers on 3EMO-IP is slightly less than that on MO-IP. The better thermal stability of 3EMO can protect the fiber on pressboard surface at high temperature.

(4) The difference in gas production properties between 3EMO-IP and MO-IP concentrates on C_2H_2 and total hydrocarbon gases. C_2H_2 is the main gas produced by surface flashover, which accounts for 43.38% of the total dissolved gases in 3EMO after 20 times flashover. The contents of H_2 and total hydrocarbon gases also have huge increases with flashover times. Besides, the diagnosis method of surface

flashover fault for mineral oil transformer is also suitable for the 3-elemnt mixed oil-insulation cellulose pressboard system, which promote the engineering application of the 3-elemnt mixed insulation oil.

REFERENCES

[1] J. Liu, X. Fan, Y. Zhang, H. Zheng, H. Yao, C. Zhang, Y. Zhang, and D. Li, "A novel universal approach for temperature correction on frequency domain spectroscopy curve of transformer polymer insulation," *Polymers*, vol. 11, no. 7, p. 1126, Jul. 2019.

[2] N. Liang, R. Liao, M. Xiang, Y. Mo, and Y. Yuan, "Influence of amine compounds on the thermal stability of paper-oil insulation," *Polymers*, vol. 10, no. 8, p. 891, Aug. 2018.

[3] J. Liu, X. Fan, H. Zheng, Y. Zhang, C. Zhang, B. Lai, J. Wang, G. Ren, and E. Zhang, "Aging condition assessment of transformer oil-immersed cellulosic insulation based upon the average activation energy method," *Cellulose*, vol. 26, no. 6, pp. 3891–3908, Apr. 2019.

[4] X. Wang, C. Tang, B. Huang, J. Hao, and G. Chen, "Review of research progress on the electrical properties and modification of mineral insulating oils used in power transformers," *Energies*, vol. 11, no. 3, p. 487, Feb. 2018.

[5] J. Li, H. C. Liang, B. X. Du, and Z. H. Wang, "Surface functional graded spacer for compact HVDC gaseous insulated system," *IEEE Trans. Dielectr. Electr. Insul.*, vol. 26, no. 2, pp. 664–667, Apr. 2019.

[6] U. M. Rao, Y. R. Sood, and R. K. Jarial, "Performance analysis of alternate liquid dielectrics for power transformers," *IEEE Trans. Dielectr. Electr. Insul.*, vol. 23, no. 4, pp. 2475–2484, Aug. 2016.

[7] L. Yang, B. Deng, R. Liao, C. Sun, and M. Zhu, "Influence of vegetable oil on the thermal aging rate of kraft paper and its mechanism," *IEEE Trans. Dielectr. Electr. Insul.*, vol. 18, no. 3, pp. 692–700, Jul. 2011.

[8] M. A. G. Martins, "Vegetable oils, an alternative to mineral oil for power transformers- experimental study of paper aging in vegetable oil versus mineral oil," *IEEE Elect. Insul. Mag.*, vol. 26, no. 6, pp. 7–13, Nov. 2010.

[9] J. Carcedo, I. Fernandez, A. Ortiz, F. Delgado, C. Renedo, and A. Arroyo, "Quantitative study on the aging of kraft paper in vegetable oils," *IEEE Elect. Insul. Mag.*, vol. 32, no. 6, pp. 29–35, Nov./Dec. 2016.

[10] S. Singha, R. Asano, G. Frimpong, C. C. Claiborne, and D. Cherry, "Comparative aging characteristics between a high oleic natural ester dielectric liquid and mineral oil," *IEEE Trans. Dielectrics Electr. Insul.*, vol. 21, no. 1, pp. 149–158, Feb. 2014.

[11] H. B. H. Sitorus, R. Setiabudy, S. Bismo, and A. Beroual, "Jatropha curcas methyl ester oil obtaining as vegetable insulating oil," *IEEE Trans. Dielectr. Electr. Insul.*, vol. 23, no. 4, pp. 2021–2028, Aug. 2016.

[12] R. Liao, S. Liang, L. Yang, J. Hao, and J. Li, "Comparison of ageing results for transformer oil-paper insulation subjected to thermal ageing in mineral oil and ageing in retardant oil," *IEEE Trans. Dielectr. Electr. Insul.*, vol. 19, no. 1, pp. 225–232, Feb. 2012.

[13] R. J. Liao, P. Guo, N. R. Zhou, H. H. Xia, Y. D. Lin, and H. B. Liu, "The thermal aging characteristics of the new anti-aging mixed insulation oil-pressboard insulation," *Trans. China Electrotech. Soc.*, vol. 30, no. 22, pp. 222–230, Nov. 2015.

[14] K. Takahashi, K. Miyagi, and R. Hanaoka, "Negative discharge response of blend oil (ester-based insulating oil with aging mineral oil) in a non-uniform field," in *Proc. IEEE 19th Int. Conf. Dielectric Liquids (ICDL)*, Jun. 2017, pp. 1–4.

[15] A. Beroual, H. B. H. Sitorus, R. Setiabudy, and S. Bismo, "Comparative study of AC and DC breakdown voltages in Jatropha methyl ester oil, mineral oil, and their mixtures," *IEEE Trans. Dielectr. Electr. Insul.*, vol. 25, no. 5, pp. 1831–1836, Oct. 2018.

[16] R. Liao, D. Feng, J. Hao, L. Yang, J. Li, Q. Wang, and S. Zhang, "Thermal and electrical properties of a novel 3-element mixed insulation oil for power transformers," *IEEE Trans. Dielectr. Electr. Insul.*, vol. 26, no. 2, pp. 610–617, Apr. 2019.

[17] D. Feng, J. Hao, R. Liao, X. Chen, L. Cheng, and M. Liu, "Comparative study on the thermal-aging characteristics of cellulose insulation polymer immersed in new three-element mixed oil and mineral oil," *Polymers*, vol. 11, no. 8, p. 1292, Aug. 2019.

[18] A. Denat, "High field conduction and prebreakdown phenomena in dielectric liquids," *IEEE Trans. Dielectr. Electr. Insul.*, vol. 13, no. 3, pp. 518–525, Jun. 2006.

[19] J. Jadidian, M. Zahn, N. Lavesson, O. Widlund, and K. Borg, "Surface flashover breakdown mechanisms on liquid immersed dielectrics," *Appl. Phys. Lett.*, vol. 100, no. 17, p. 1327, Apr. 2012.

[20] M. P. Wilson, S. J. Macgregor, M. J. Given, I. V. Timoshkin, M. A. Sinclair, K. J. Thomas, and J. M. Lehr, "Surface flashover of oil-immersed dielectric materials in uniform and non-uniform fields," *IEEE Trans. Dielectr. Electr. Insul.*, vol. 16, no. 4, pp. 1028–1036, Aug. 2009.

[21] C. Thirumurugan, G. B. Kumbhar, and R. Oruganti, "Effects of impurities on surface discharges at synthetic ester/cellulose board," *IEEE Trans. Dielectr. Electr. Insul.*, vol. 26, no. 1, pp. 64–71, Feb. 2019.

[22] A. Beroual and L. Kebbabi, "Influence of the voltage waveform and hydrostatic pressure on morphology and final length of discharges propagating over solid-liquid interfaces," *IEEE Trans. Dielectr. Electr. Insul.*, vol. 16, no. 6, pp. 1574–1581, Dec. 2009.

[23] A. Beroual, V.-H. Dang, M.-L. Coulibaly, and C. Perrier, "Investigation on creeping discharges propagating over pressboard immersed in mineral and vegetable oils under AC, DC and lightning impulse voltages," *IEEE Trans. Dielectr. Electr. Insul.*, vol. 20, no. 5, pp. 1635–1640, Oct. 2013.

[24] R. Liao, J. Hao, L. Yang, S. Liang, and Z. Ma, "Simulation and experimental study on frequency-domain dielectric spectroscopy of oil-paper insulation for transformers," *Proc. CSEE*, vol. 30, no. 22, pp. 113–119, 2010.

[25] P. Zou, J. Li, C. Sun, R. Liao, and Z. Zhang, "Influences of moisture content on insulation properties of vegetable insulating oil," *High Voltage*, vol. 37, no. 7, pp. 1627–1633, 2011.

[26] J.-H. Choi, S.-H. Kim, K. Jang, M. Hikita, and S.-H. Lee, "Finite-element analysis for surface discharge due to interfacial polarization at the oil-nanocomposite interface," *IEEE Trans. Magn.*, vol. 54, no. 3, Mar. 2018, Art. no. 7204904.

[27] *Mineral Oil-Filled Electrical Equipment in Service-Guidance on the Interpretation of the Dissolved and Free Gases Analysis*, Standard, IEC 60599, 2015.

XIN CHEN was born in Shaanxi, China, in 1994. He received the B.Eng. degree from Chongqing University, China, in 2017, where he is currently pursuing the master's degree with the College of Electrical Engineering. His research interest includes the new type of insulation material.

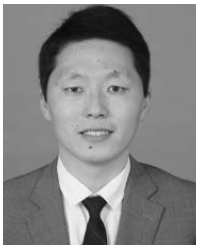

JIAN HAO was born in Hebei, China, in 1984. He received the B. Eng. and B. Economic degrees from the College of Electrical Engineering and College of Economics and Business Administration, Chongqing University, China, in 2007, and the doctor's degree from the College of Electrical Engineering, Chongqing University, in 2012, where he is currently working. His research interests include ageing mechanism, dielectric response, and space charge characteristics of oil-paper insulation systems.

RUIJIN LIAO was born in Sichuan, China, in 1963. He received the M.S. and Ph.D. degrees in electrical engineering from Xi'an Jiaotong University, China, and Chongqing University, China, respectively, where he has been a Professor with Electrical Engineering College, since 1999. He is author/coauthor of one book and over 90 journal and international conferences. His research interests include on-line monitoring of insulation condition and fault diagnosis for high voltage apparatus.

JIAN LI was born in Shanxi, China, in 1971. He received the Ph.D. degree in electrical engineering from Chongqing University, China, in 2001, where he is currently with the College of Electrical Engineering. He engaged in online monitoring and intelligent fault diagnosis of electrical equipment, insulation aging, and electrical insulation materials. He is author/coauthor of over 80 journal and international conferences.

LIJUN YANG was born in Sichuan, China, in 1980. She received the M.S. and Ph.D. degrees in electrical engineering from Chongqing University, China, in 2004 and 2009, respectively, where she is currently with the College of Electrical Engineering. Her major research interests include online detection of insulation condition of electrical devices, partial discharges, and insulation fault diagnosis for high voltage equipment.

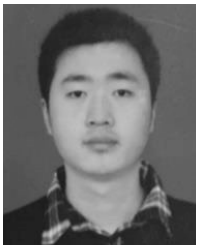

DAWEI FENG was born in Sichuan, China, in 1992. He received the master's degree in electrical engineering from Chongqing University, Chongqing, China, in 2017, where he is currently pursuing the Ph.D. degree with the Electrical Engineering College. His major research interests include insulation fault diagnosis for high voltage equipment and property of insulation oil.